Chemical Engineering Science 282 (2023) 119219

Contents lists available at ScienceDirect

Chemical Engineering Science

journal homepage: www.elsevier.com/locate/ces

Membrane process design for biohydrogen purification with simultaneous CO_2 capture: Feasibility and techno-economic assessment

Wenqi Xu [a], Arne Lindbråthen [a], Saravanan Janakiram [b], Luca Ansaloni [b], Linfeng Lei [c], Liyuan Deng [a,*]

[a] Department of Chemical Engineering, Norwegian University of Science and Technology (NTNU), Trondheim NO-7491, Norway
[b] Department of Sustainable Energy Technology, SINTEF Industry, 0373 Oslo, Norway
[c] State Key Laboratory of Chemical Engineering, School of Chemical Engineering, East China University of Science and Technology, 130 Meilong Road, Shanghai 200237, China

ARTICLE INFO

Keywords:
Membrane process
Dark fermentative biohydrogen
Hydrogen purification: CO_2 capture
Techno-economic assessment

ABSTRACT

In this work, a membrane separation process is designed and optimized to purify dark fermentative biohydrogen by removing CO_2. A CO_2-selective PVAm-based nanocomposite membrane was selected considering its high CO_2/H_2 separation performance and unique features suitable for the process. We tested the membrane performances under the separation conditions to provide a more accurate simulation basis. Several design scenarios were investigated. A two-stage process with a recycle stream is determined as the optimal design, in which the specific cost for purifying H_2 to 99.5 vol% with H_2 loss of <10% reaches only 0.156 \$/Nm^3. The techno-economic feasibility study of biohydrogen purification with simultaneous CO_2 capture was also performed through an alternative design by introducing a 3rd-stage using the same membrane or an H_2-selective membrane. Adding a 3rd-stage membrane can capture and purify CO_2 as a side product of various purities, which further decreases the H_2 loss, leading to additional economic benefits.

1. Introduction

Carbon emissions from energy generation and the consequent increase of CO_2 concentration in the atmosphere are believed to be the direct culprit of climate change and environmental degradation, such as global warming and rising sea level (Cartwright, 2021). As the primary source of CO_2 emission is using fossil fuels for energy generation (Norahim et al., 2018), the global energy structure can be shifted to non-carbon-based fuels to reduce CO_2 emissions. Hydrogen, as a clean energy carrier and energy vector, has been used in various applications and is considered a promising alternative to traditional fossil fuels. Today, the most common hydrogen production is from natural gas-based integrated gasification combined cycle (IGCC) processes through energy-intensive separation steps at elevated operating temperatures and pressures. Recently, although usually in a much smaller size than IGCC, a renewable and sustainable process to produce biohydrogen through biomass conversion by dark fermentation has attracted increasing attention (Nanda et al., 2015; Younas et al., 2022). The conversion of biomass provides high energy content biofuels. The dark fermentation process operates under much lower temperatures and pressures and is easy to operate with low energy consumption (Nanda et al., 2015; Sarangi and Nanda, 2020; Younas et al., 2022).

H_2 production streams from both IGCC and dark fermentation contain a large amount of CO_2 and are saturated with water (Lee et al., 2011). Purifying H_2 from the water-saturated CO_2/H_2 mixture is challenging. Traditional H_2 purification technologies, such as pressure swing adsorption (PSA), cryogenic process, and absorption, are mostly energy intensive (Bernardo et al., 2020; Li et al., 2015) and have high specific cost for H_2 purification, especially when a small-sized plant is considered. Moreover, the presence of water reduces the separation efficiency of the above-mentioned H_2 purification processes; thus, water should be removed as a necessary pre-treatment step before the separation when using these technologies.

Membrane technology was introduced for CO_2 and H_2 separation to purify biohydrogen from dark fermentation in this work. Although membrane separation is an emerging technology in hydrogen purification, it has shown enormous potential due to its small footprint, low operating and capital cost, few chemical additives, process flexibility,

* Corresponding author.
E-mail address: liyuan.deng@ntnu.no (L. Deng).

https://doi.org/10.1016/j.ces.2023.119219
Received 9 July 2023; Received in revised form 20 August 2023; Accepted 23 August 2023
Available online 3 September 2023

and high energy efficiency, especially for small to medium size plants (Czyperek et al., 2010; Han and Ho, 2020; Huang et al., 2022). Two different categories of membranes can be used for CO_2/H_2 separation, namely, H_2-selective membranes or CO_2-selective membranes. H_2-selective membranes allow H_2 to transport through membranes and be purified at the permeate side at low pressures, such as in palladium membranes (Atsonios et al., 2014; Sazali et al., 2020), polymeric membranes (Han and Ho, 2021b; Huang et al., 2022), and carbon membranes (Dai et al., 2023; Salleh and Ismail, 2015). Franz et al. evaluated the H_2 purification process for an IGCC plant by process simulation using H_2-selective membranes and CO_2-selective membranes, respectively. They found that, due to the selectivity limitation, a single-stage process using a CO_2-selective membrane cannot reach a separation efficiency of >85%. To achieve the production specification, two or even three stages are needed (Franz and Scherer, 2010). Lei et al. reported a process using an H_2-selective carbon membrane for CO_2 and H_2 separation from an IGCC plant (Lei et al., 2021). Later, He et al. studied the use of the same H_2-selective carbon membrane on biohydrogen from dark fermentation (He et al., 2021).

Since the molecular size of H_2 (2.9 Å) is significantly smaller than that of CO_2 (3.3 Å) (Pal and Agarwal, 2021), so far, most developed membranes for CO_2/H_2 separation are H_2-selective; only a few CO_2-selective membranes have been reported in the literature. CO_2-selective membranes for H_2 purification are usually based on materials of high CO_2 solubility selectivity, but most of them still exhibited moderate CO_2/H_2 separation performances since H_2 is nearly the smallest gas (Han and Ho, 2021b). Some ether oxygen-rich polymeric membranes were reported for excellent CO_2/H_2 selectivity but require very low separation temperature, i.e., −20 °C (Lin et al., 2006), implying that a very energy-intensive pre-cooling step is needed to reach the optimal separation conditions. On the other hand, CO_2-selective membranes following the facilitated transport mechanism have been reported with exceptional CO_2/H_2 separation performance by Ho and co-workers, especially at elevated temperatures (at >100 °C) (Yang et al., 2020; Zhao and Ho, 2012). Facilitated transport membranes contain CO_2-affinity carriers in the membrane matrix that reversibly react with CO_2, often in the presence of water (Hägg and Deng, 2015; Rafiq et al., 2016; Rivero et al., 2023). The hydration reactions enable a reverse selectivity against the size difference, allowing CO_2 transport through the membrane while H_2 stays and is enriched at the retentate side. The process design and techno-economic feasibility of this type of membranes have been studied for H_2 purification from the IGCC process syngas (Chen et al., 2021; Han and Ho, 2021a), but have not yet been considered for biohydrogen purification of dark fermentation streams where the process size is small and the separation is under moderate conditions (Lee et al., 2011).

In our previous study, a polyvinylamine (PVAm)-based facilitated transport membrane incorporated with polyvinyl alcohol (PVA)-grafted-graphene oxide (GO) (PVAm/(PVA-GO)) was developed (Xu et al., 2023). A CO_2/H_2 selectivity of 22 and CO_2 permeability 61.6 Barrer (10 vol% CO_2 in H_2 with saturated water) under 1.7 bar at 25 °C was reported. The performance overcomes the CO_2/H_2 Upper-bound (Lin et al., 2006) and is among the best-performing CO_2-selective CO_2/H_2 separation membranes under similar testing conditions except for some reported works at elevated temperatures (Ansaloni et al., 2015; Tong and Ho, 2017; Yang et al., 2020; Zhao et al., 2014; Zhao and Ho, 2012), showing great potential for the purification of fermentative biohydrogen under mild separation conditions. It is worthy mentioning that the water vapour favors the facilitated transport membranes such as the membrane under discussion.

The current work aims to design and optimize a highly efficient process for biohydrogen purification using a CO_2-selective membrane, i.e., PVAm/(PVA-GO) membrane, and to conduct the techno-economic feasibility study of the designed process. Since the H_2 streams from both IGCC and dark fermentation are water-saturated, and the PVAm/(PVA-GO) membrane works better in the water-swollen state, no pre-treatment is required to remove water vapor for CO_2-selective membranes, which simplifies the process. Thus, the application of facilitated transport membranes is expected to be more advantageous. In addition, using the CO_2-selective membrane process can keep the purified biohydrogen on the high-pressure side of the membrane, which is beneficial to the further utilization of the produced hydrogen. However, to the best of the authors' knowledge, few studies on fermentative biohydrogen purification using CO_2-selective membranes have been reported.

In this work, membrane separation processes were designed and evaluated by simulation studies. The performance data of the PVAm/PVA-GO membrane under the given conditions were systematically tested for a more accurate investigation of the process. The performance data were tested with a fully humidified CO_2/H_2 mixture with compositions of 10 vol% CO_2 in H_2 and 40 vol% CO_2 in H_2 at temperatures of 25 °C to 75 °C, reflecting the expected 1st- and 2nd-stage feed conditions and the dark fermentation conditions, respectively. Membrane separation processes were then designed and simulated with ChemBrane (a user-customized membrane module solver) integrated with Aspen HYSYS using the performance data at the given conditions. Both single-stage and two-stage membrane processes were investigated to check the process potentials. The process simulation targets at H_2 purity of 99.5% as pure fuel with <10 % H_2 loss, with which a low cost of biohydrogen production was achieved by using the 2-stage PVAm/(PVA-GO) membrane process with recycle. Based on the findings, a 3rd-stage membrane unit was also introduced to purify the enriched CO_2 to achieve simultaneous CO_2 capture; sensitivity analysis of CO_2 purity as the target product purity was studied in this case. Cost estimation of the process was performed, including operating expenditure (OPEX) and capital expenditure (CAPEX) related to the operating parameter of each membrane stage, which was further related to the membrane areas and power consumptions (vacuum pump and compressor included). With the addition of a 3rd-stage membrane unit, the final products of the process include both high-purity H_2 with a much lower H_2 loss and high-purity CO_2 as a side product, leading to a low specific cost for green H_2 purification with simultaneous CO_2 capture for negative carbon emission.

2. Experimental

2.1. Membrane preparation

The PVAm/PVA-GO nanocomposite membranes were fabricated following the procedure detailed in (Xu et al., 2023). A brief description is given here for the readers' convenience. 3.0 wt% PVAm aqueous solution was purified from Lupamin® 9095 (BASF AG, Germany) and diluted. Graphene oxide (GO, <100 mesh, from LayerOne, Norway) was dissolved into DI water with sodium hydroxide (NaOH, 97 %, from Sigma-Aldrich, Norway) to adjust the pH to 10 to prepare 1 mg/mL water suspension. GO solution was sonicated to ensure exfoliation and a thorough dispersion (Janakiram et al., 2020). Polyvinyl alcohol (PVA, Mw: 85,000–124,000, 87–89 % hydrolyzed, from Sigma-Aldrich, Norway) was dissolved into DI water and the according amount of dispersed GO solution was added into PVA solution with stirring under 60 °C to yield PVA-GO solutions with the concentration of PVA and GO in the solution as 0.034 wt% and 0.046 wt%, respectively. Afterward, the CO_2-selective nanocomposite flat-sheet membranes were coated on commercial polysulfone ultrafiltration membranes as membrane substrates (GR40PP, 20 k MWCO, from Alfa Laval Nordic AS) using a dip coating machine (KCV NIMA, Biolin Scientific, Finland). The coated PVAm/PVA-GO membranes were then dried under room condition (approx 6 h) and treated at 90 °C for 1 h.

2.2. Membrane performance testing

The prepared PVAm/(PVA-GO) membranes were tested using fully humid mixed gases of two compositions, i.e., 10 vol% CO_2 in H_2, and 40

vol% CO_2 in H_2 with feed pressure as 1.7 bar at varying temperatures, from 25 °C to 75 °C. The permeation testing rig is custom-made, as described in (Dai et al., 2019). The sweep gas is nitrogen or argon at approx. 1 bar with two different set-ups to verify the CO_2/H_2 separation performance. The concentrations of CO_2 and H_2 from the sweep/permeate side were measured by a pre-calibrated gas chromatograph (GC, 490 Micro GC, Agilent). The permeance of CO_2 ($\frac{P_i}{l}$, $1\ GPU = 0.001217\ \frac{mol}{kPa \bullet hour \bullet m^2}$) can be obtained according to Eq. (1):

$$\frac{P_i}{l} = \frac{N_{perm}(1 - y_{H_2O})y_i}{A(p_{i,feed} - p_{i,perm})} \quad (1)$$

where P_i is the permeability of CO_2 and N_{perm} is the total permeate flow rate that was measured using a bubble flow meter, y_{H_2O} is the mole fraction of water in the permeate flow calculated according to the measured relative humidity and the vapor pressure ($\Phi = \frac{p_{H_2O}}{p^*_{H_2O}}$, which Φ is relative humidity, p_{H_2O} is the partial pressure of water vapor, and $p^*_{H_2O}$ is the saturation vapor pressure of water at a given temperature) according to the testing condition, y_i is the molar fraction of gas specie *i* in the permeate side, A is the effective membrane area, and $p_{i,feed}$ and $p_{i,perm}$ is the partial pressure of gas specie *i* in the feed and permeate side.

3. Process simulation methods

3.1. Process description

The main components of the raw product stream from dark fermentation are H_2 and CO_2, with a small percent of CH_4 (as an impurity here) and traces of other impurities, and saturated with water (Ghimire et al., 2015). It should be noted that the concentrations of impurities can be tailored by applying different conditions and/or different microorganisms in dark fermentation reactors (Guo et al., 2010). Thus, only components H_2, CO_2, and water are considered in this work. Temperatures in the streams out of any dark fermentation tank vary from 25 °C to 80 °C according to the species of microorganisms (Lee et al., 2011). The conditions of a typical dark fermentation product stream are summarized in Table 1 (Lee et al., 2011). In order to produce green H_2 as high-quality fuel, the produced H_2 purity was set to be 99.5 vol%, and the H_2 loss was controlled to be below 10 vol% (He et al., 2021; Lei et al., 2021).

The water-saturated gas stream from dark fermentation needs to be pressurized for separation. Afterward, the pressurized gas is cooled down to the given operating temperature (from 25 °C to 75 °C) and fed into the membrane unit. Single-stage and two-stage CO_2-selective facilitated transport membrane systems based on the PVAm/(PVA-GO) membrane are designed, as illustrated in Fig. 1.

As shown in Fig. 1 (a), the single-stage membrane system contains a compressor (K-1) to increase the pressure from 1 bar to 1.7 bar (the pressure of 1.7 bar was determined through experiment as mentioned before and applied throughout the study), a heat exchanger (E-1) to decrease the stream temperature to the operating temperature after the compression, and a vacuum pump at the permeate side. Fig. 1 (b) presents the two-stage process, where the 1st-stage and the 2nd-stage are designed to control the H_2 loss and H_2 purity, respectively, by the Adjust Unit (ADJ), in which the membrane area was used as an adjustable variable and H_2 loss and H_2 purity were set as the target variables. The two-stage membrane process consists of two CO_2-selective membranes, two compressors (K-1 and K-2), two heat exchangers (E-1 and E-2), and two vacuum pumps at the permeate side of the respective membrane units. The gas stream from the fermenter combined with the recycle was fed into the compressor (K-1) to reach the separation pressures. The enriched H_2 from the 1st-stage membrane's (M−1) retentate side is then directly sent as the feed stream to the 2nd-stage membrane unit (M−2) for the ultimate biohydrogen purification to produce purified H_2. The permeate stream from the 2nd-stage membrane unit contains a large amount of hydrogen and is recycled back to the 1st-stage to avoid high H_2 loss. Compressor (K-2) is applied in the recycle stream to compress the gas stream back to 1.0 bar to mix with the feed gas stream.

Table 1
Dark fermentation biohydrogen product stream conditions.

Parameters		Bio reactor conditions	Simulation basis
Temperature, °C		25 ~ 80	25, 35, 45, 55, 65, 75
Pressure, bar		1	1
Gas composition, vol.%	CO_2	30–40	40
	H_2	40–60	60
	CH_4	0–5	0

In this work, only membrane configurations in the asymmetric cascade layout (the retentate flow from the 1st-stage feeding into the 2nd-stage), not the symmetric cascade (the permeate flow fed into the 2nd-stage), were considered for two reasons: (1) the membrane is CO_2-selective and based on facilitated transport; thus, feeding the permeate stream (enriched with CO_2) into the 2nd-stage will cause carrier saturation in the facilitated transport membranes and consequently operate below the optimal performance; and (2) if the 1st-stage permeate stream (vacuum) is fed into the 2nd-stage, additional compression is needed, adding extra capital cost and energy consumption.

3.2. Simulation basis and general assumptions

Table 2 shows the simulation basis for the process based on the outlet flow conditions of dark fermentation (e.g., feed gas flow rate and temperature) and experimental data (feed and permeate side pressures).

As temperature plays a critical role in the facilitated transport mechanism, the selected membranes were experimentally evaluated at various temperatures in the expected range of the dark fermentation conditions to provide a more accurate simulation basis. The designed processes were simulated by Aspen HYSYS interfaced with a user-customized module, ChemBrane (Deng and Hägg, 2010). The simulation results based on ChemBrane show excellent consistency compared with experimental data, as reported by (Chu et al., 2019). The Peng–Robinson property package in Aspen HYSYS was used. Cross-flow, co-current and counter-current flow are considered in the ChemBrane. Cross-flow is typical for a spiral-wound module, while counter-current is typically used for hollow fibers.

The following assumptions were made to simplify the simulation:

- The membrane modules are assumed as hollow fiber modules with the counter-current flow.
- The compression ratio over each compressor stage is limited to 3.0
- A vacuum pump was used in the permeate side for all the membrane units, and it was simulated as an adiabatic compressor train.
- All compressors are modeled to have an adiabatic efficiency of 0.75.
- Heat exchanger costs are not included in the study.

As an example of the simulation using ChemBrane interfaced with Aspen HYSYS®, a flow sheet is shown in Fig. 2 for the designed 2nd-stage process configuration. The 1st humidifier was set to simulate the water saturated feed stream, and the 2nd humidifier was set to increase the relative humidity to to optimal condition for CO_2/H_2 gas separation. The cost of 2nd humidifier is not included in this work.

3.3. Cost model

A rough economic evaluation was performed for the process design and optimization to minimize the capital and operating costs. As vacuum pumps, compressors, and membrane units dominate the total cost in the membrane separation system, the capital costs were estimated only on these dominating equipment and membrane units. The capital cost is based on the 2021 Chemical Engineering Plant Cost Index (CEPCI), which gives a value of 708, and CAPCOST 2017, a software

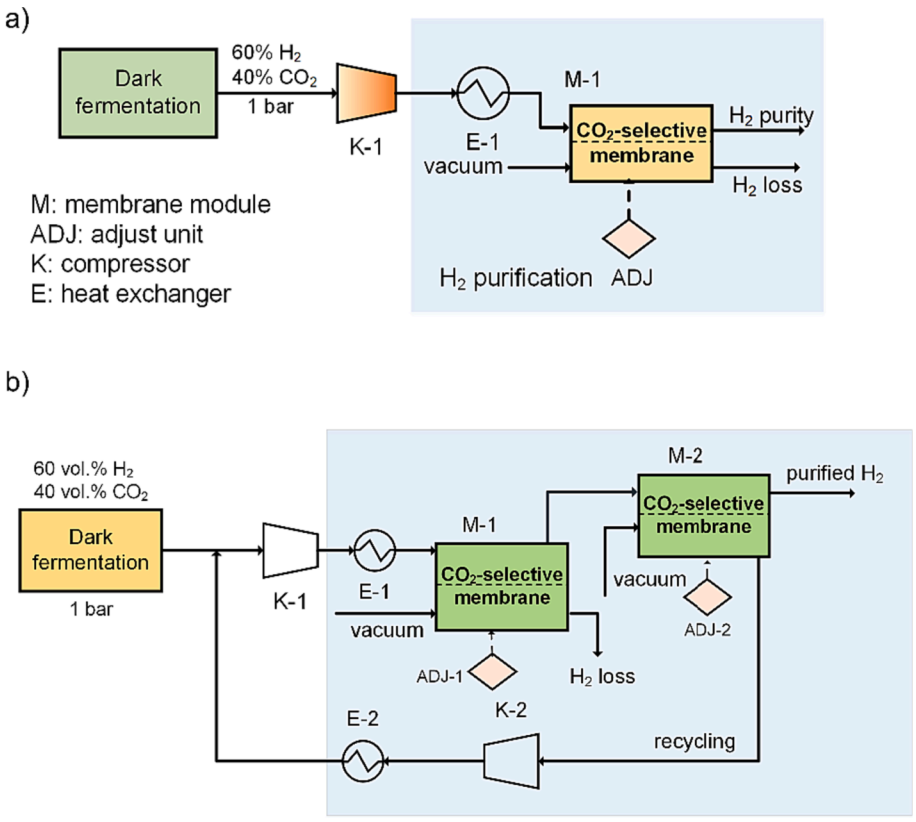

Fig. 1. Process flow diagram of a) a single-stage and b) a two-stage membrane system for biohydrogen purification.

Table 2
Simulation parameters for the biohydrogen purification process.

Feed gas flow rate (dry base), m^3(STP)/h	3000
Temperature, °C	25 ~ 75
Feed pressure, bar	1.7
Permeate pressure, mbar	400

based on (Turton et al., 2008), was used for capital cost estimation. Carbon steel rotary compressors (18 kW ~ 900 kW) were used for this application. It is worth mentioning that under relatively low temperatures with high H_2 purity, hydrogen embrittlement should be considered when selecting materials for equipment and pipes. But, in this work, the hydrogen embrittlement issue was not considered to simplify the capital cost calculation.

The purchase cost, C_p^0, of rotary compressors is estimated by Eq. (2),

$$log_{10}C_p^0 = K_1 + K_2 log_{10}(Q) + K_3[log_{10}(Q)]^2 \quad (2)$$

where Q is the power consumption of compressors, and K_1, K_2, and K_3 are constants of rotary compressors for cost estimation as 5.0355 (K_1), −1.8002(K_2), and 0.8525(K_3), respectively (Turton et al., 2008). The bare module cost, C_{BM}, is calculated for compressors cost estimation based on the purchase cost of rotary compressors and a bare module factor, F_{BM}, as shown in Eq. (3) (Turton et al., 2008).

$$C_{BM} = C_p^0 F_{BM} \quad (3)$$

The total module cost, C_{TM}, is estimated by the bare module cost, and the grassroots cost, C_{GR}, can be further evaluated by the total module cost, as illustrated in Eqs. (4) and (5).

$$C_{TM} = 1.18\sum_{i=}^{n} C_{BM} \quad (4)$$

$$C_{GR} = C_{TM} + 0.5\sum_{i=}^{n} C_{BM,i}^0 \quad (5)$$

where n is the number of equipment and $C_{BM,i}^0$ is the bare module cost in

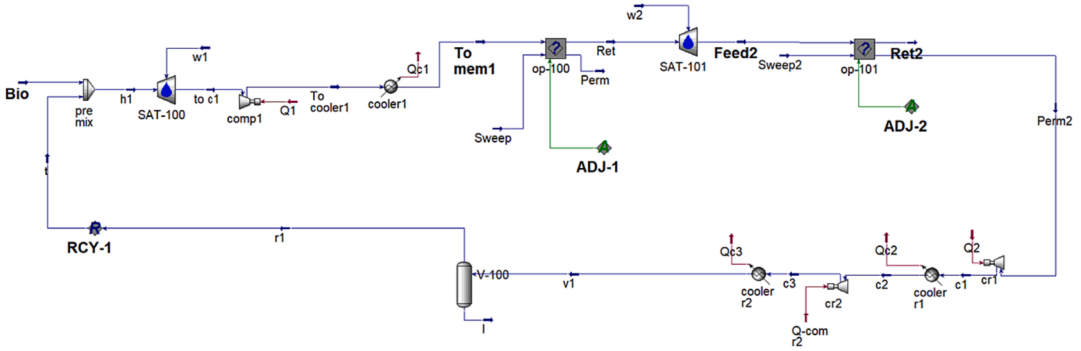

Fig. 2. Flow sheet of the 2nd-stage membrane process in Aspen HYSYS®.

the base condition. For the membrane unit, 50 $/m^2 is the estimated price of PVAm/(PVA-GO) membranes, including material costs for membranes and modules and the installation cost. Annual capital-related cost (CRC) for the whole system can be evaluated to be 20% of the C_{GR} and 28% of the membrane module cost, C_M. To simplify the cost estimation, only electricity and labor cost are considered as operating expenditures (OPEX), where the electricity cost is 0.05 $/kWh, and labor cost is 17 $/h, which is the average standard all over the world (He et al., 2021; Lei et al., 2021) with the total operating hour of 7500 h/year. The specific cost of H_2 purification ($/Nm^3 H_2 produced) can be calculated by Eq. (6).

$$H_2 specific cost = \frac{CRC + OPEX}{annual H_2 productivity} \quad (6)$$

In this work, the lifetimes of the membrane, equipment, and project are assumed as 5 years, 20 years, and 20 years, respectively.

4. Results and discussion

4.1. Gas separation performance

The membrane performances of the CO_2-selective PVAm/(PVA-GO) membranes are given in Table 3, including two feed compositions (CO_2/H_2 mixtures of 40% CO_2 and 10% CO_2) at varying temperatures. The experimental data are given in the Supporting Information (Fig. S1). The H_2-selective carbon molecular sieving membrane performances (50% CO_2) at varied temperatures are listed in Table 4. The CO_2 and H_2 permeances presented in Tables 3 and 4 at the given temperature are based on the linear fitting data from the experimental results.

For CO_2-selective membranes (see Table 3), when the feed gas containing 40 vol% CO_2 in H_2, CO_2 permeance decreases, and H_2 permeance increases with increasing temperature. This trend shows that, under relatively high CO_2 concentrations, the effect of CO_2 sorption on gas permeation is more significant than diffusion, which decreases with increasing temperature. However, when the feed gas contains only 10 vol% CO_2 in H_2 (Table.3), both CO_2 permeance and H_2 permeance increase with increasing temperature, implying that the effect of diffusion becomes more significant in the gas transport through the membrane.

It needs to be noted that due to the measurement limitation in the concentration of water at the permeate side, the water permeance of the membranes could not be determined by the current experiments. Therefore, it is assumed that the water permeance in a membrane is the same as the permeance of the favorable gas through the membrane, a method adapted from the literature (He et al., 2021; Lei et al., 2021), i.e., the water permeance is assumed the same as the H_2 permeance in H_2-selective membranes and as the CO_2 permeance in CO_2-selective membranes.

All the gas separation performance results from the experimental study were obtained with a standard deviation lower than 10%. Thus, the deviations are not presented in the Tables.

Table 3
Membrane performances of the CO_2-selective PVAm/(PVA-GO) membrane.

Temperature (°C)	40 vol% CO_2 in H_2		10 vol% CO_2 in H_2	
	CO_2 permeance (GPU)	H_2 permeance (GPU)	CO_2 permeance (GPU)	H_2 permeance (GPU)
25	58.6	3.2	14.3	0.8
35	53.4	3.8	21.4	1.5
45	48.9	4.6	31.1	2.6
55	45	5.4	44.4	4.4
65	41.6	6.3	62	7.3
75	38.7	7.3	84.8	11.7

Table 4
Membrane performances of H_2-selective carbon molecular sieving membranes, tested with 50 vol% H_2 in CO_2 (He et al., 2021).

Temperature (°C)	H_2 permeance (GPU)	CO_2 permeance (GPU)
25	27.3	0.8
35	34	1.1
45	41.9	1.3
55	50.8	1.5
65	61	1.8
75	72.4	2.1

4.2. Process optimization

4.2.1. Single-stage membrane process

In the single-stage membrane process, the raw biohydrogen stream from dark fermentation is fed directly to the PVAm/(PVA-GO) membrane unit after being compressed to 1.7 bar. As the performance of the selected facilitated transport membrane varies significantly with the temperature, the influence of feed temperature, which is controlled by fermentative temperature from 25 °C to 75 °C, was investigated by simulation. The required membrane area was adjusted to achieve an H_2 loss of < 10 %. The obtained H_2 purities at given temperatures are presented in Fig. 3. With increasing operating temperature in the single stage, the achieved H_2 purity decreases. This is expected as the membrane exhibits higher CO_2 permeance but decreasing CO_2/H_2 selectivity with increasing temperature for the CO_2/H_2 mixture of 40% CO_2. Therefore, the optimal temperature for a single-stage membrane is determined to be at 25 °C when targeting high purity, where the highest H_2 purity of 87 vol% is obtained.

The operating temperature of 25 °C was used in further studies of the dependence of H_2 purity on the H_2 loss. Fig. 4 shows the relationship between H_2 loss and H_2 purity in a single-stage membrane system (the blown dataset) and the membrane area required to control the given H_2 loss (the blue dataset). As shown in the figure, the H_2 purity (retentate side) decreases with a lower H_2 loss (controlled at the permeate side), and the required membrane area at a given H_2 loss shows a similar trend as expected. In the case of achieving a lower H_2 loss, less H_2 transports through a smaller membrane area; hence the retentate H_2 purity decreases. For a higher H_2 purity, more CO_2 must permeate through the membrane, which requires a higher membrane area, thus leading to a higher H_2 loss. Therefore, there is a clear trade-off between H_2 loss and

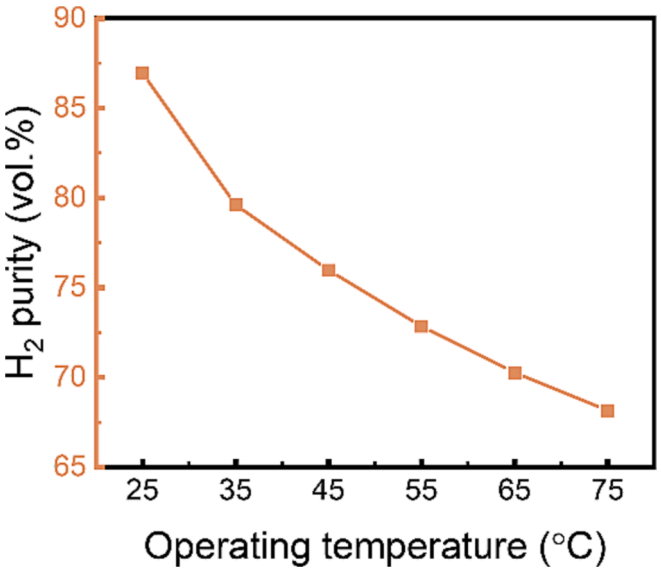

Fig. 3. Effect of single-stage feed temperature on the H_2 purity with fixed H_2 loss as 10 %.

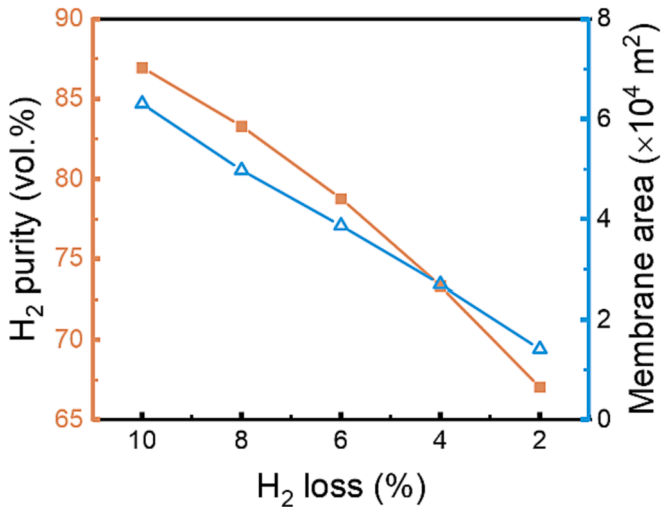

Fig. 4. Effects of H_2 loss on membrane area (blue line) and the trade-off between H_2 purity and H_2 loss (brown line) in the single-stage membrane process, at 25 °C, 1.7 bar.

H_2 purity in a single-stage membrane system, and one more stage is needed for biohydrogen purification to achieve the required high purity of H_2 (99.5 vol%) and low H_2 loss (<10%).

4.2.2. *Two-stage membrane process*

Since the operating temperature significantly influences gas separation performances of the PVAm/(PVA-GO) membrane, it will certainly further affect the capital cost and specific cost of the H_2 purification process. Thus, the operating temperatures of each membrane unit are optimized through process simulation and techno-economic analysis with fixed H_2 loss and H_2 purity. According to the experimental data with the feed gas of 40 vol% CO_2 in H_2, a higher operating temperature results in a lower CO_2 permeance and simultaneous loss in selectivity. Since membranes of a lower CO_2 permeance lead to an increase in the required membrane area for the separation to meet the H_2 purity requirement, an additional membrane area is required to compensate for the permeance loss. Consequently, the CRC, determined by the membrane module cost, becomes a function of the operating temperature. Hence, the operating temperature of the membrane units can be optimized to minimize the capital cost and specific cost of H_2 purification.

The effect of operating temperature on membrane area, power consumption, and costs is studied in the designed two-stage, CO_2-selective membrane process (Marked as scenario A) in this work. The total H_2 loss of 10% and H_2 purity of 99.5 vol% (dry base) are fixed as the targets; only the temperatures in the 2nd-stage are allowed to vary. Table 5 lists the details of scenario A for the optimizations of operating temperatures of membrane units in the two-staged membrane system, where in case A1, the 2nd-stage temperature is fixed to be 25 °C while the 1st-stage membrane is allowed to vary to optimize the 1st-stage temperature. In the case of A2, the optimized 1st-stage temperature based on case A1 will be fixed to study the effect of temperature change in the 2nd-stage membrane module.

When the feed stream temperature of the 1st-stage membrane increases from 25 °C to 75 °C, the process can be easily implemented since the fermentative temperature of dark fermentation is from 25 °C to 75 °C (Lee et al., 2011).

When the 1st-stage operating temperature increases, the membrane area of the 1st-stage slightly changes, first decreasing then increasing at 55 °C, while that of the 2nd-stage increases notably and almost linearly. Since the CO_2 permeance of the membrane increases and CO_2/H_2 selective decreases with increasing temperature, the operating temperature shows a significant influence on the membrane area in the 1st-stage membrane unit. However, the 1st-stage membrane area is also affected by the recycle stream; increasing the operating temperature of the 1st-stage membrane unit increases the needed ratio for the recycle stream and thus increases the membrane area. The sum of the two effects makes a slightly curved downtrend of the 1st-stage membrane area with temperature, but the overall power consumption increases monotonously due to the much larger amount of the recycle stream to meet the requirement of H_2 purity and H_2 loss, as presented in Fig. 5 (a) and (b). As the membrane unit cost dominates the CRC, the CRC value reaches the minimum, and the specific cost of H_2 production follows the same trend, as shown in Fig. 5 (c). Thus, the optimal operating temperature of the 1st-stage feed stream is set to be 25 °C, and the specific cost of purifying H_2 at this temperature is 0.266 \$/Nm^3.

After the optimal feed stream temperature of the 1st-stage is determined to be 25 °C, the effect of operating temperature at the 2nd-stage was investigated by process simulation with the 1st-stage temperature fixed as 25 °C and the 2nd-stage temperature varying from 25 ~ 75 °C, as the scenario A2. It should be pointed out that the feed gas mixture in the 2nd stage has a composition of approx. 10 vol% CO_2 in H_2. Thus, the data set for the 10 vol% CO_2 in H_2 listed in Table 3 was used for the 2nd-stage simulation.

Fig. 6 shows the effect of the 2nd-stage operating temperature on membrane area (a), the power consumption (b), and CRC, OPEX, specific cost of H_2 purification (c). As can be seen, the membrane area of the 1st-stage is almost constant with increasing 2nd-stage temperatures, but the effect on the 2nd-stage membrane area is significant, showing a notable declining trend with increasing temperature, which is opposite to the trend of the membrane area with the increasing 1st-stage temperature. The opposite effects of temperature on CO_2 permeance using the feeds of 10 vol% CO_2 in H_2 and 40 vol% CO_2 in H_2 are believed to have caused different trends. For the feed stream of 10 vol% CO_2 in H_2, the CO_2 permeance increases with increasing temperature; hence a higher CO_2 flow goes through the membrane, leading to increasing energy consumption for both the vacuum pump at the permeate side in the 2nd-stage and the compressor to pressurize the increasing recycle stream back to 1 bar to mix with the outlet stream of dark fermentation. Thus, the power consumption of the process increases with increasing 2nd-stage temperature, as presented in Fig. 6 (b). As mentioned before, the cost of membrane units and compressors dominates CRC. Thus, as shown in Fig. 6 (c), the CRC cost decreases and OPEX increases (from 0.216×10^6 \$ to 0.335×10^6 \$) with increasing 2nd-stage temperature due to the increase in power consumption.

Similarly, when the operating temperature of 2nd-stage increases, the specific cost of H_2 purification also decreases, but it can be minimized by balancing CRC and OPEX. Based on these factors as discussed above, the optimal feed temperature of 2nd-stage is determined to be 55 °C, which reaches the minimum H_2 specific purification cost of 0.156 \$/Nm^3. Surprisingly, the CO_2 loss under the optimal condition is only 0.67 %, and CO_2 purity has already been around 87 vol% (dry base). Thus, the two-stage CO_2-selective membrane system designed for biohydrogen purification has a huge potential to obtain high purity of CO_2 as a side-product. The data on effects of flow rate, operating temperature, and H_2 purification cost in Scenario A1 and A2 are provided in the Supporting information in Table S1.

Table 5
Scenario A for optimizations of operating temperatures in membrane units.

Scenario	T, °C **1st-stage**	T, °C **2nd-stage**	P_{feed}, bar	H_2 purity, % (dry base)	H_2 loss, %
A1	25 ~ 75	25	1.7	99.5	10
A2	Optimized	25 ~ 75			

4.2.3. *Three-stage membrane process simulation*

Processes with two-stage configurations are the most commonly used multi-stage processes, as the complexity of variable control and the extra

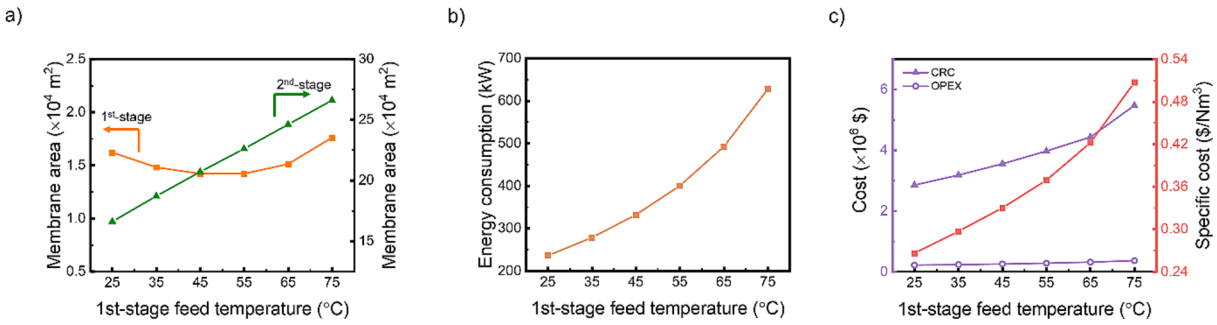

Fig. 5. Effects of the 1st-stage feed temperature on a) membrane area (orange line: 1st-stage, and green line: 2nd-stage), b) power consumption of major equipment, and c) CRC, OPEX, and specific cost.

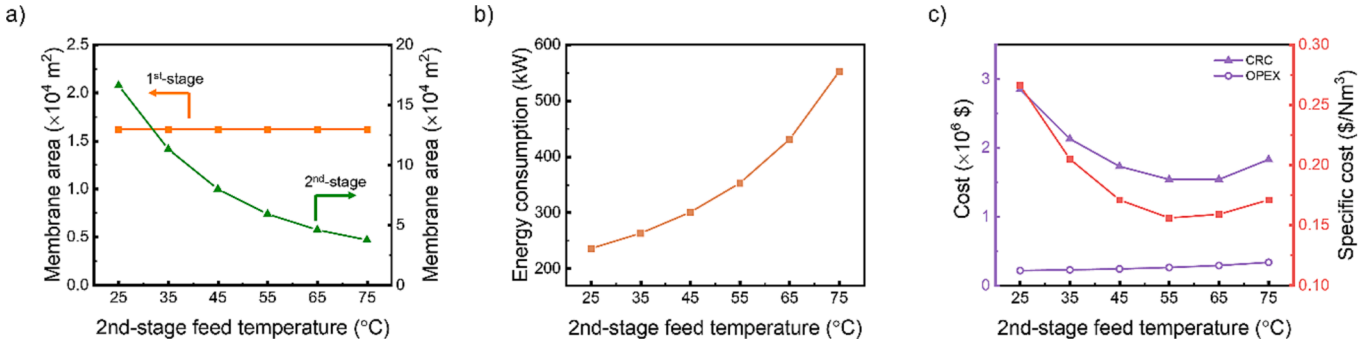

Fig. 6. Effects of 2nd-stage feed temperature on a) membrane area, b) power consumption of major equipment, and c) CRC, OPEX, and specific cost.

costs limit the applications of processes with processes of three or more stages unless the additional stages result in significant benefits. Nevertheless, adding an extra stage can further purify CO_2 from the 2nd-stage H_2 purification process as a by-product, which could be rewarding both economically and from the environmental perspective, i.e., achieving negative carbon emissions. In general, CO_2 capture requires the process to meet specifications for CO_2 storage or utilization, e.g., CO_2 purity of $>$ 90% and CO_2 capture rate of 90%, and the price of CO_2 depends on its purity. Higher CO_2 purity usually makes more value, thus selling at a higher price.

A 3rd-stage membrane unit was introduced to the optimized two-stage membrane processes to further purify the enriched CO_2 from the permeate stream of the 1st-stage membrane to meet the CO2 capture specification. As shown in Fig. 7, three-stage membrane processes were designed. The potential of two different types of membrane in the added 3rd-stage, i.e., CO_2-selective membranes as Scenario B (Fig. 4 (a)) and H_2-selective membranes as Scenario C (Fig. 4 (b)), were investigated to find the most economical process design.

The same PVAm/(PVA-GO) membrane was used as the CO_2-selective membrane in the 3rd-stage unit as Scenario B. Since the 1st-stage permeate stream feeding into the 3rd-stage membrane module has a very high CO_2 concentration already, the permeation of the large amount of CO_2 will require a large membrane area. Thus, using an H_2-selective membrane in the 3rd stage instead could be a promising alternative considering the very low H_2 content in the feed to that stage, requiring a lower membrane area to permeate a smaller amount of H_2.

In the case of using an H_2-selective membrane as the 3rd stage membrane (Scenario C), several different types of H_2-selective membranes were compared by literature study to determine the most suitable candidate for efficient H_2/CO_2 separation (Al-Rowaili et al., 2023; Cardoso et al., 2018; Sazali, 2020). According to the literature, Palladium (Pd)-based membranes have been widely investigated and known as highly H_2 selective (Atsonios et al., 2014). However, Pd-based membranes are costly both for the materials and fabrication process. Besides, the low temperature and pressure for biohydrogen purification make H_2 hard to dissociate, causing low diffusivity and, thus, low separation efficiency. The complicated impurities from the bioreactor may poison Pd-membranes as well. Therefore, the Pd membrane was not selected in this work. Carbon membrane has also been reported for their high H_2/CO_2 selectivities (Tseng et al., 2016). Recently, Dai et al. (Dai et al., 2023) and Lei et al. (Lei et al., 2021) reported H_2-selective carbon membranes with high H_2/CO_2 selectivity, and Lei et al. have also studied the process for H_2 purification. Although the fabrication of carbon membranes is, in general, costly, Lei's study showed relatively low specific cost in processes for H_2 purification by assuming the membrane cost of 100$/m^2 (Chen et al., 2023; He et al., 2021; Lei et al., 2021). It is interesting to compare these studies with our work. Thus, the H_2-selective cellulose-based carbon membrane reported by Lei et al. was chosen as the 3rd-stage membrane unit in the current study.

As shown in Fig. 7 (a), a 3rd-stage CO_2-selective membrane unit was set up for the process as Scenario B, in which the retentate stream out of the 1st-stage membrane unit (M−1) is fed into the 2nd-stage membrane unit (M−2) to enrich H_2 as the product, and the permeate stream from the 2nd-stage was recycled to M1 to ensure low H_2 loss. The permeate side of M−1 is fed into the 3rd-stage membrane unit (M−3) with an additional compressor to increase the pressure to the 3rd-stage separation pressure. M−3 was used to enrich CO_2 as the second product in the permeate, while the retentate stream was recycled to ensure low H_2 loss. The design is different in Scenario C (see Fig. 7 (b)), where the 1st-stage membrane unit (M−1) and the 2nd-stage membrane unit (M−2) are the same, but additional condenser (C-1) before the stream feeding into the 3rd-stage membrane unit (M−3) was needed in order to remove water as water may cause a negative effect for carbon-based membranes governed by the molecular sieving mechanism. Also, enriched CO_2 is obtained at the retentate side of M−3, and the permeate side must be recycled back to M1 to avoid H_2 loss. Due to the requirement of high purity H_2 and only a small amount of CO_2 in the retentate side in M2, the resulting CO_2 driving force is low at the 2nd-stage; thus, the 1st-stage was used to control the CO_2 concentration in the fed of the 2nd-stage based on $\frac{x_{r,CO_2}}{x_{f,CO_2}} = 0.5$ (Mulder and Mulder, 1996). Adjust units (ADJ-1

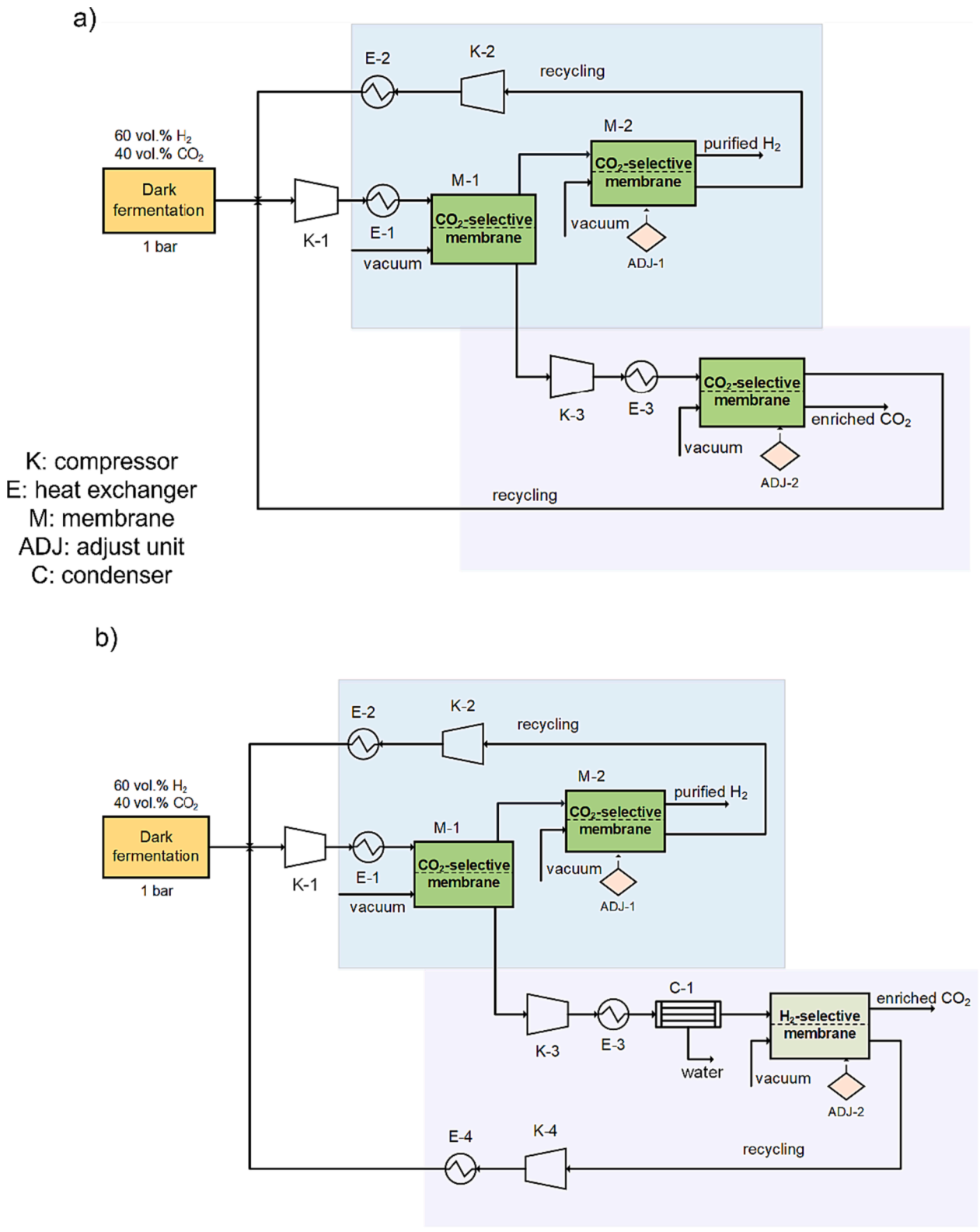

Fig. 7. Process flow diagram of three-stage membrane systems using a) CO_2-selective membrane (Scenario B) and b) using H_2-selective membrane as the 3rd-stage for biohydrogen purification (Scenario C).

and ADJ-2) were used to control H_2 purity and CO_2 purity as the adjusted variable, respectively, and membrane area was adjusted as the target variable. Due to the extra preparation procedure for carbonization compared with polymeric membranes, 100 $\$/m^2$ is assumed as the price of cellulose-based carbon membranes, including materials and modules of membranes and installation cost, the same value as given in (He et al., 2021; Lei et al., 2021).

To further investigate the feasibility of simultaneous CO_2 capture in the H_2 purification process, the proposed scenarios B and C were modelled based on the optimal condition of the two-stage system. The

techno-economic analysis for the target H_2 purity and H_2 loss, and CO_2 purity and CO_2 loss of the 3rd-stage were analyzed, as listed in Table 6, with the 1st-stage and 2nd-stage operating temperature set as 25 °C and 55 °C, respectively. Two different designs for scenarios B and C were compared, and the influence of different 3rd-stage membrane materials and operating temperatures were also investigated.

CO_2-selective membrane in the 3rd-stage (Scenario B)

By using a CO_2-selective membrane as the 3rd-stage, the 40 vol% CO_2 in H_2 data in Table 3 was used for simulation. As shown in Fig. 8 (a), the total membrane area shows a small difference at various temperatures at the 3rd-stage. According to the data for 40 vol% CO_2 in H_2, the CO_2 permeance decrease, and H_2 permeance increase with increasing operating temperature. Thus, to obtain high purity CO_2 in the 3rd-stage, a lower temperature is more favorable; Thus, a lower gas volume from the 3rd-stage retentate needs to be recycled due to the higher selectivity at a lower temperature (i.e., at 25 °C), which, in turn, results in lower power consumption for the compressor and vacuum pump, as presented in Fig. 8(b).

Since power consumption dominates OPEX, the operating temperature (feed flow temperature) can be optimized by tuning the optimal operation temperatures to minimize the specific cost. Fig. 9 demonstrates the effect of the 3rd-stage feed temperature on CRC, OPEX, and specific cost. Due to the slight increase in membrane area and power consumption, the CRC and OPEX increase slightly, and consequently, the specific cost of H_2 purification follows the same trend. Thus, the optimal specific cost of purifying 99.5 vol% H_2 (≪10% H_2 loss) and 90 vol% CO_2 (<1% CO_2 loss) is 0.189 $ per Nm^3 of purified hydrogen when the 3rd-stage operating at the optimal temperature of 45 °C, or roughly in the range of 35–55 °C. Moreover, if the carbon credit income of the captured CO_2 as a by-product of hydrogen production is available and included, the hydrogen purification cost could be even lower.

H_2-selective membrane in the 3rd-stage (Scenario C)

By using an H_2-selective membrane as the 3rd stage, a carbon membrane based on the data given in Table 4 was applied to investigate the temperature influence. The data, such as flow rate, operating temperature, and H_2 purification cost of Scenario B and C, are summarized in the Supporting Information in Table S2. One of the advantages of cellulose-based carbon membranes is that both H_2/CO_2 selectivity and H_2 and CO_2 permeance increase with increasing temperature. The analysis of the operating temperature over an expanded range of 25–75 °C was investigated in order to obtain a relatively high purity of CO_2 (90 vol%, dry base) with low H_2 loss and CO_2 loss. As shown in Fig. 10 (a), membrane areas of the 1st-stage and 2nd-stage are almost constant, and the membrane area of the 3rd-stage slightly decreases with increasing 3rd-stage operating temperature since H_2 permeance increased and less membrane area is needed to obtain the requirement of CO_2 purity. More energy may be needed for a large amount of recycling for the permeate of the 3rd-stage. Nevertheless, according to the simulation, the increased total power consumption is negligible, and hence the influence of the 3rd-stage temperature on OPEX can be neglected, as shown in Fig. 10 (b) for the CRC, OPEX, and specific cost plots. CRC has shown a small decrease with increasing operating temperature, causing a slightly decreasing specific cost for H_2 purification. Based on the factors, under 75 °C, the specific cost for H_2 purification reaches the lowest value at 0.173 $/$Nm^3$ if the heating and water removal costs are not included. Compared with using a CO_2-selective membrane as the 3rd-stage membrane system, using an H_2-selective membrane gives only a little lower specific cost for purifying H_2, but with only a<10% difference for this case when the CO_2 purity is set to be 90%. Taking into account the pre-treatment steps needed when using a carbon membrane, there is no benefit to changing the 3rd-stage membrane to an H_2-selective carbon membrane when the targeted CO_2 purity is only 90%.

It is worth mentioning that current biohydrogen processes are at relatively small scales. In order to be close to the real industrial condition, a relatively low total feed flow (gas stream from dark fermentation) was used in these simulations for fermentative hydrogen purification. Therefore, the vacuum pump sizes are too small to use rotary compressors in CAPEX estimation, so the selling price of SMC Vacuum Pump from RS Norway (~770 $/piece) was used to calculate the CAPEX based on the Eq. (3).

4.3. Sensitivity analysis of CO_2 purity in the three-stage process

Based on the above optimized operating temperature for the three-stage membrane separation system, the sensitivity analysis of the effects of CO_2 purity as different products (90–99.95%) was analyzed with fixed H_2 purity (99.5 vol%), H_2 loss < 10 %, and CO_2 loss < 1 %, as listed in Table 6 marked with a star (*). Since scenarios B and C show similar specific costs (<10% difference), the sensitivity analysis of CO_2 purity with a CO_2-selective membrane as the 3rd-stage membrane or an H_2-selective membrane as the 3rd-stage membrane should be investigated. Since the selectivity of CO_2/H_2 in the CO_2-selective membrane is limited, according to a preliminary study, achieving a higher CO_2 purity of > 95% using the CO_2-selective membrane as the 3rd-stage is too costly. Thus, only using the H_2-selective membrane in the 3rd stage (scenario C*) was investigated on the techno-economic feasibility of obtaining CO_2 of different purities as side products.

Fig. 11 summarizes the sensitivity of the required CO_2 purity on the process design. As shown in Fig. 11 (a), when increasing the operating temperature of the 3rd-stage from 25 to 75 °C, the total membrane area slightly decreases, from 82 600 to 79 600 m^2 for 90 vol% CO_2 purity and from 98 800 to 88 300 m^2 for 95 vol% CO_2 purity. High CO_2 purity of 99.5% and above requires a much larger membrane area. According to the carbon membrane's gas separation performance (see Table 4), increasing temperature leads to the increase of both gas permeances and H_2/CO_2 selectivity. Therefore, increasing the operating temperature of the 3rd stage decreases the 3rd-stage and total membrane area, which directly reduces CRC, as shown in Fig. 11 (b). Since OPEX is only considered the influence of electricity and labor cost in this work, and in the sensitivity analysis, the differences in power consumption on each concentration with different temperatures are small, the OPEX difference can be neglected in the analysis. Fig. 11 (c) shows the specific cost for H_2 purification increases for producing high-purity CO_2.

5. Conclusions

A two-stage membrane system was designed using a CO_2-selective membrane (PVAm/(PVA-GO)) to obtain high-purity H_2 as high-quality biofuel from biomass through dark fermentation. According to the simulation results, using the PVAm/PVA-GO membrane for biohydrogen purification is economically feasible; Only ~ 0.156 $ is needed for the purification of each Nm^3 of biohydrogen to reach 99.5 vol% purity, leaving CO_2 (~87%) as a by-product.

To further purify CO_2 to meet the CO_2 capture specification for CO_2

Table 6
Simulation parameters for scenario B and C.

Scenario	Membrane type	T, °C			H_2 purity, %	H_2 loss, %	CO_2 purity, %
		1st-stage	2nd-stage	3rd-stage			
B	CO_2-selective	25	55	25–75	99.5	<10	90
C	H_2-selective						(90–99.5)*

*Data used for sensitivity study of CO_2 purities.

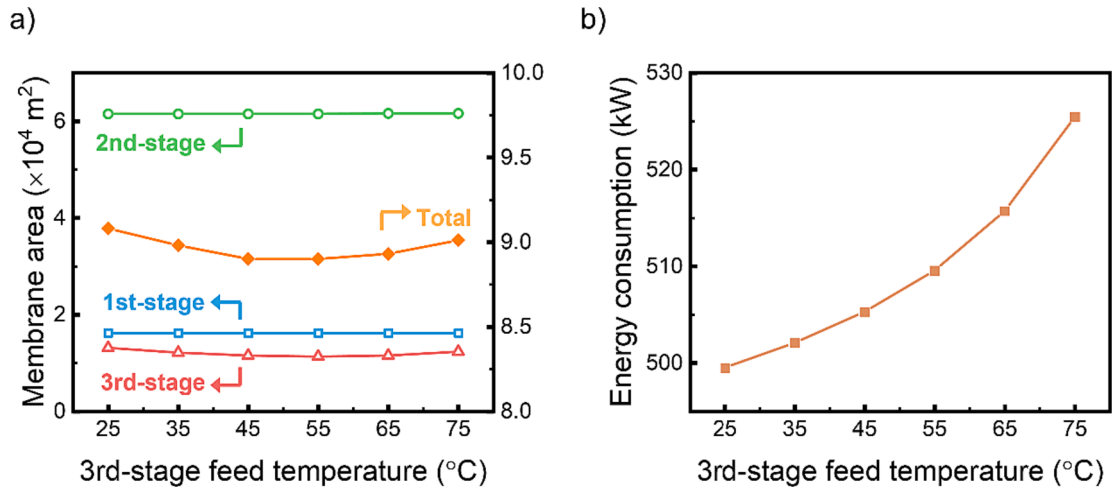

Fig. 8. Effects of 3rd-stage feed temperature on the a) membrane area (CO_2-selective) and b) power consumption of major equipment.

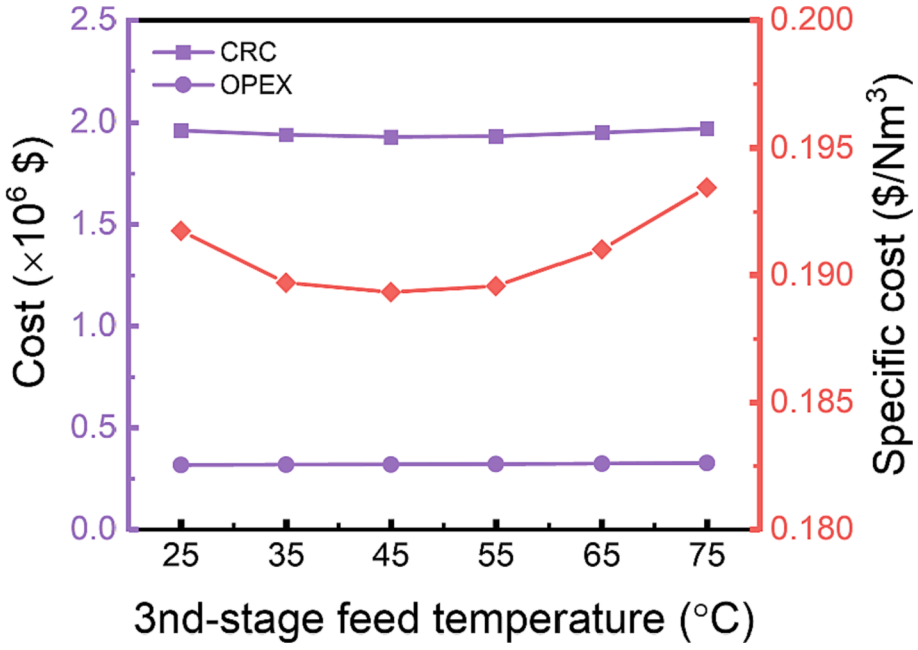

Fig. 9. Effects of 3rd-stage (CO_2-selective) feed temperature on CRC, OPEX and specific cost.

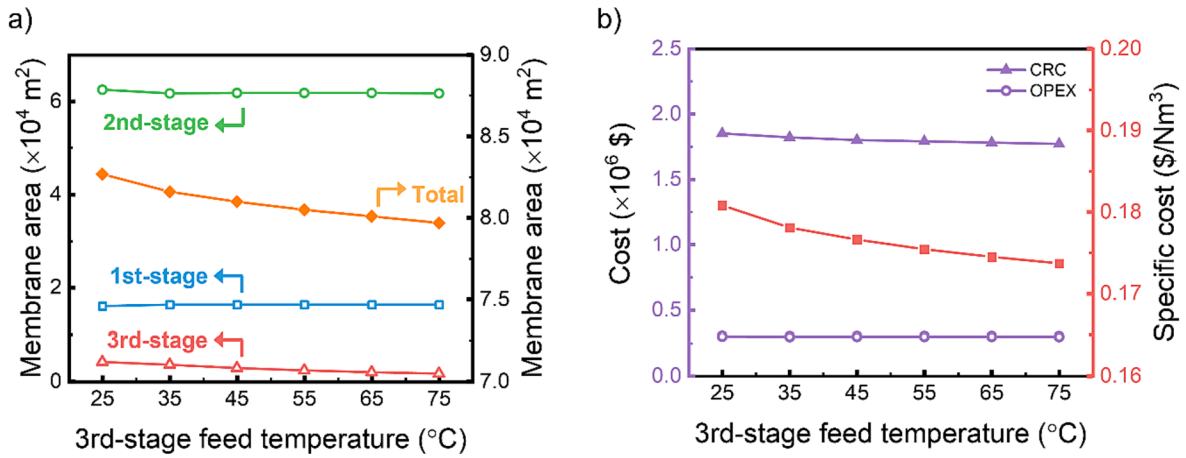

Fig. 10. Effects of 3rd-stage (H_2-selective) feed temperature on a) membrane area and power consumption, and b) CRC, OPEX and specific cost of producing H_2.

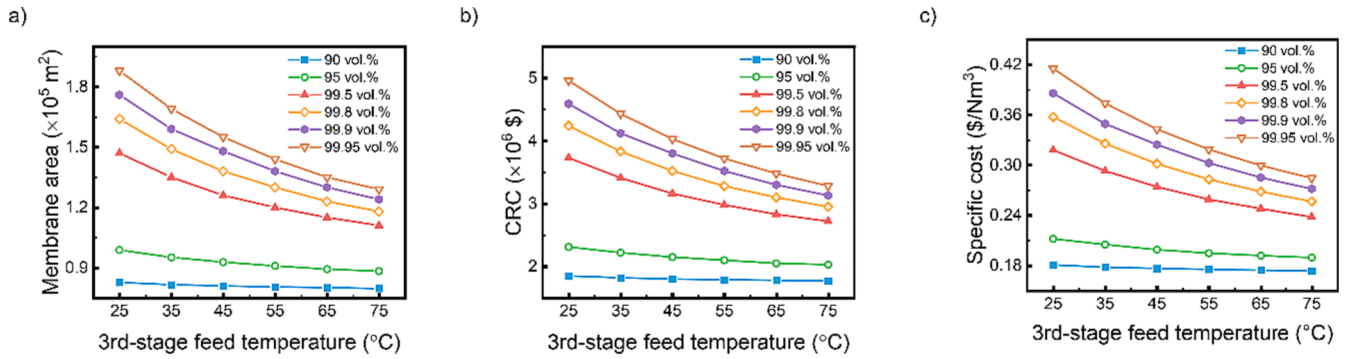

Fig. 11. Sensitivity analysis of CO_2 purity on a) membrane area, b) CRC, and c) specific cost of H_2 production in scenario C*.

storage or utilization and achieve negative carbon emission, a 3rd-stage membrane was introduced to the two-stage process using either a CO_2-selective membrane unit (scenario B) or an H_2-selective membrane as the 3rd-stage (scenario C and C*), with which CO_2 capture with different purities for storage or various utilization applications can be achieved at a low cost. In the three-stage process, the specific cost for H_2 purification can take in the selling income of two products, H_2 and CO_2, and the selling price of the higher purity of CO_2 also increases, which will partially offset the increased production cost. As the selling profits of H_2 as high quality fuel and high purity CO_2 with different applications were not included in this work, the actual profit was underestimated.

In future work, costs for the pre-treatment steps in using H_2-selective carbon membranes must be added to the process design and economic analysis, and a more detailed economic analysis and cash flow should be conducted by taking into account the CO_2 income when the market prices of CO_2 at various purities are available. Applying membranes with improved performance may result in a lower capital cost, such as using our recently reported H_2-selective carbon membrane with superior CO_2/H_2 separation performance (Dai et al., 2023).

CRediT authorship contribution statement

Wenqi Xu: Methodology, Formal analysis, Validation, Investigation, Writing – original draft, Visualization. **Arne Lindbråthen:** Writing – review & editing. **Saravanan Janakiram:** Writing – review & editing. **Luca Ansaloni:** Writing – review & editing, Funding acquisition. **Linfeng Lei:** Writing – review & editing. **Liyuan Deng:** Conceptualization, Writing – review & editing, Supervision, Project administration, Funding acquisition.

Declaration of Competing Interest

The authors declare that they have no known competing financial interests or personal relationships that could have appeared to influence the work reported in this paper.

Data availability

Data will be made available on request.

Acknowledgements

This work is part of the FaT H2 project supported by the Research Council of Norway (No. 294533).

Appendix A. Supplementary data

Experimental data of CO_2 and H_2 permeance and the simulation and economic data of Scenarioes A1, A2, B and C. Supplementary data to this article can be found online at https://doi.org/10.1016/j.ces.2023.119219.

References

Al-Rowaili, F.N., Khaled, M., Jamal, A., Zahid, U., 2023. Mixed matrix membranes for H2/CO2 gas separation- a critical review. Fuel 333, 126285.
Ansaloni, L., Zhao, Y.N., Jung, B.T., Ramasubramanian, K., Baschetti, M.G., Ho, W.S.W., 2015. Facilitated transport membranes containing amino-functionalized multi-walled carbon nanotubes for high-pressure CO2 separations. J. Membr. Sci. 490, 18–28.
Atsonios, K., Panopoulos, K., Doukelis, A., Koumanakos, A., Kakaras, E., Peters, T., van Delft, Y., 2014. Introduction to palladium membrane technology. Palladium Membrane Technology for Hydrogen Production, Carbon Capture and Other Applications: Principles, Energy Production and Other Applications. Elsevier, 1-21.
Bernardo, G., Araújo, T., da Silva Lopes, T., Sousa, J., Mendes, A., 2020. Recent advances in membrane technologies for hydrogen purification. Int. J. Hydrogen Energy 45 (12), 7313–7338.
Cardoso, S.P., Azenha, I.S., Lin, Z., Portugal, I., Rodrigues, A.E., Silva, C.M., 2018. Inorganic Membranes for Hydrogen Separation. Sep. Purif. Rev. 47 (3), 229–266.
Cartwright, E.D., 2021. "Code Red"—Recent IPCC Report Warns Time is Running Out on Climate Change. Climate Energy 38 (3), 11–12.
Chen, K.K., Han, Y., Tong, Z.i., Gasda, M., Ho, W.S.W., 2021. Membrane processes for CO2 removal and fuel utilization enhancement for solid oxide fuel cells. J. Membr. Sci. 620, 118846.
Chen, D., Wang, K., Yuan, Z., Lin, Z., Zhang, M., Li, Y., Tang, J., Liang, Z., Li, Y., Chen, L., Li, L., Huang, X., Pan, S., Zhu, Z., Hong, Z., He, X., 2023. Boosting membranes for CO2 capture toward industrial decarbonization. Carbon Capture Sci. Technol. 7, 100117.
Chu, Y.H., Lindbrathen, A., Lei, L.F., He, X.Z., Hillestad, M., 2019. Mathematical modeling and process parametric study of CO2 removal from natural gas by hollow fiber membranes. Chem. Eng. Res. Des. 148, 45–55.
Czyperek, M., Zapp, P., Bouwmeester, H.J.M., Modigell, M., Ebert, K., Voigt, I., Meulenberg, W.A., Singheiser, L., Stöver, D., 2010. Gas separation membranes for zero-emission fossil power plants: MEM-BRAIN. J. Membr. Sci. 359 (1-2), 149–159.
Dai, Z., Deng, J., Yu, Q., Helberg, R.M.L., Janakiram, S., Ansaloni, L., Deng, L., 2019. Fabrication and Evaluation of Bio-Based Nanocomposite TFC Hollow Fiber Membranes for Enhanced CO(2) Capture. ACS Appl. Mater. Interfaces 11 (11), 10874–10882.
Dai, Z., Guo, H., Deng, J., Deng, L., Yan, J., Spontak, R.J., 2023. Carbon molecular-sieve membranes developed from a Tröger's base polymer and possessing superior gas-separation performance. J. Membr. Sci. 680, 121731.
Deng, L., Hägg, M.-B., 2010. Techno-economic evaluation of biogas upgrading process using CO2 facilitated transport membrane. Int. J. Greenhouse Gas Control 4 (4), 638–646.
Franz, J., Scherer, V., 2010. An evaluation of CO2 and H2 selective polymeric membranes for CO2 separation in IGCC processes. J. Membr. Sci. 359 (1-2), 173–183.
Ghimire, A., Frunzo, L., Pirozzi, F., Trably, E., Escudie, R., Lens, P.N.L., Esposito, G., 2015. A review on dark fermentative biohydrogen production from organic biomass: Process parameters and use of by-products. Appl. Energy 144, 73–95.
Guo, X.M., Trably, E., Latrille, E., Carrère, H., Steyer, J.-P., 2010. Hydrogen production from agricultural waste by dark fermentation: A review. Int. J. Hydrogen Energy 35 (19), 10660–10673.
Hägg, M.-B., Deng, L., 2015. Membranes in gas separation, in: 2 (Ed.), Handbook of Membrane Separations: Chemical, Pharmaceutical, Food, and Biotechnological Applications. CRC press, pp. 143-180.
Han, Y., Ho, W.S.W., 2020. Recent advances in polymeric facilitated transport membranes for carbon dioxide separation and hydrogen purification. J. Polym. Sci. 58 (18), 2435–2449.
Han, Y., Ho, W.S.W., 2021a. Facilitated transport membranes for H2 purification from coal-derived syngas: A techno-economic analysis. J. Membr. Sci. 636, 119549.
Han, Y., Ho, W.S.W., 2021b. Polymeric membranes for CO2 separation and capture. J. Membr. Sci. 628, 119244.

He, X., Lei, L., Dai, Z., 2021. Green hydrogen enrichment with carbon membrane processes: Techno-economic feasibility and sensitivity analysis. Sep. Purif. Technol. 276, 119346.
Huang, L., Xing, Z., Zhuang, X., Wei, J., Ma, Y., Wang, B., Jiang, X., He, X., Deng, L., Dai, Z., 2022. Polymeric membranes and their derivatives for H2/CH4 separation: State of the art. Sep. Purif. Technol. 297, 121504.
Janakiram, S., Martín Espejo, J.L., Yu, X., Ansaloni, L., Deng, L., 2020. Facilitated transport membranes containing graphene oxide-based nanoplatelets for CO2 separation: Effect of 2D filler properties. J. Membr. Sci. 616, 118626.
Lee, D.-J., Show, K.-Y., Su, A.y., 2011. Dark fermentation on biohydrogen production: Pure culture. Bioresour. Technol. 102 (18), 8393–8402.
Lei, L., Lindbråthen, A., Hillestad, M., He, X., 2021. Carbon molecular sieve membranes for hydrogen purification from a steam methane reforming process. J. Membr. Sci. 627, 119241.
Li, P.Y., Wang, Z., Qiao, Z.H., Liu, Y.N., Cao, X.C., Li, W., Wang, J.X., Wang, S.C., 2015. Recent developments in membranes for efficient hydrogen purification. J. Membr. Sci. 495, 130–168.
Lin, H., Van Wagner, E., Freeman, B.D., Toy, L.G., Gupta, R.P., 2006. Plasticization-enhanced hydrogen purification using polymeric membranes. Science 311 (5761), 639–642.
Mulder, M., Mulder, J., 1996. Basic principles of membrane technology. Springer science & business media.
Nanda, S., Azargohar, R., Dalai, A.K., Kozinski, J.A., 2015. An assessment on the sustainability of lignocellulosic biomass for biorefining. Renew. Sustain. Energy Rev. 50, 925–941.
Norahim, N., Yaisanga, P., Faungnawakij, K., Charinpanitkul, T., Klaysom, C., 2018. Recent Membrane Developments for CO2 Separation and Capture. Chem. Eng. Technol. 41, 211–223.
Pal, N., Agarwal, M., 2021. Advances in materials process and separation mechanism of the membrane towards hydrogen separation. Int. J. Hydrogen Energy 46 (53), 27062–27087.
Rafiq, S., Deng, L., Hägg, M.-B., 2016. Role of Facilitated Transport Membranes and Composite Membranes for Efficient CO2 Capture – A Review. ChemBioEng Rev. 3 (2), 68–85.
Rivero, J.R., Nemetz, L.R., Da Conceicao, M.M., Lipscomb, G., Hornbostel, K., 2023. Modeling gas separation in flat sheet membrane modules: Impact of flow channel size variation. Carbon Capture Sci. Technol. 6, 100093.
Salleh, W., Ismail, A.F., 2015. Carbon membranes for gas separation processes: Recent progress and future perspective. J. Membr. Sci. Res. 1, 2–15.
Sarangi, P.K., Nanda, S., 2020. Biohydrogen Production Through Dark Fermentation. Chem. Eng. Technol. 43 (4), 601–612.
Sazali, N., 2020. A Short Review on Separation of H2/CO2 using Polymer Membrane. J. Adv. Res. Fluid Mech. Therm. Sci. 69, 174–182.
Sazali, N., Mohamed, M.A., Salleh, W.N.W., 2020. Membranes for hydrogen separation: a significant review. Int. J. Adv. Manuf. Technol. 107 (3-4), 1859–1881.
The Chemical Engineering Plant Cost Index - Chemical Engineering.
Tong, Z., Ho, W.S.W., 2017. New sterically hindered polyvinylamine membranes for CO2 separation and capture. J. Membr. Sci. 543, 202–211.
Tseng, H.-H., Wang, C.-T., Zhuang, G.-L., Uchytil, P., Reznickova, J., Setnickova, K., 2016. Enhanced H2/CH4 and H2/CO2 separation by carbon molecular sieve membrane coated on titania modified alumina support: Effects of TiO2 intermediate layer preparation variables on interfacial adhesion. J. Membr. Sci. 510, 391–404.
Turton, R., Bailie, R.C., Whiting, W.B., Shaeiwitz, J.A., 2008. Analysis, synthesis and design of chemical processes. Pearson Education.
Xu, W., Lindbråthen, A., Janakiram, S., Ansaloni, L., Deng, L., 2023. Enhanced CO2/H2 separation by GO and PVA-GO embedded PVAm nanocomposite membranes. J. Membr. Sci. 671, 121397.
Yang, Y., Han, Y., Pang, R., Ho, W.S.W., 2020. Amine-Containing Membranes with Functionalized Multi-Walled Carbon Nanotubes for CO2/H2 Separation. Membranes (Basel) 10, 333.
Younas, M., Shafique, S., Hafeez, A., Javed, F., Rehman, F., 2022. An Overview of Hydrogen Production: Current Status, Potential, and Challenges. Fuel 316, 123317.
Zhao, Y.N., Ho, W.S.W., 2012. Steric hindrance effect on amine demonstrated in solid polymer membranes for CO2 transport. J. Membr. Sci. 415, 132–138.
Zhao, Y., Jung, B.T., Ansaloni, L., Ho, W.W., 2014. Multiwalled carbon nanotube mixed matrix membranes containing amines for high pressure CO2/H2 separation. J. Membr. Sci. 459, 233–243.